Stabilization of Gas-Distribution Instability in Single-Point Dual Gas Lift Wells

Gisle Otto Eikrem, SPE, **Ole Morten Aamo,** and **Bjarne A. Foss,** Norwegian U. of Science and Technology

Summary

While casing-heading instability in single gas lift wells has attracted a lot of attention, gas-distribution instability in *dual* gas lift wells has not. In this paper, we present a simple, nonlinear dynamic model that is shown to capture the essential dynamics of the gas-distribution instability despite the complex nature of two-phase flow. Using the model, stability maps are generated showing regions of stable and unstable settings for the production valves governing the produced flows from the two tubings. Optimal steady-state production is shown to lie well within the unstable region, corresponding to a gas distribution between the production tubings that cannot be sustained without automatic control. A simple control structure is suggested that successfully stabilizes the gas-distribution instability in simulations and, more importantly, in laboratory experiments.

Introduction

Artificial lift is a common technique to increase tail-end production from mature fields, and injection of gas (gas lift) rates among the most widely used of such methods. Gas lift can induce severe production flow oscillations because of casing-heading instability, a phenomenon that originates from dynamic interaction between injection gas in the casing and the multiphase fluid in the tubing. The fluctuating flow typically has an oscillation period of a few hours and is distinctly different from short-term oscillations caused by hydrodynamic slugging. The casing-heading instability introduces two production-related challenges. Average production is decreased compared to a stable flow regime, and the highly oscillatory flow puts strain on downstream equipment.

Reports from industry as well as academia suggest that automatic control (feedback control) is a powerful tool to eliminate casing-heading instability and increase production from gas lift wells (Kinderen et al. 1998; Jansen et al. 1999; Dalsmo et al. 2002; Boisard et al. 2002; Hu and Golan 2003; Eikrem et al. 2003; Aamo et al. 2005). Automatic control may or may not require downhole measurements. If downhole information is needed by the controller, the use of soft-sensing techniques may alleviate the need for downhole measurements. In Aamo et al. (2005), downhole pressure is estimated on line using a simple dynamic model and measurements at the wellhead only. The estimated pressure is in turn used in a controller for stabilizing the casing-heading instability.

Understanding and predicting under which conditions a gas lift well will exhibit flow instability is important in every production-planning situation. This problem has been addressed by several authors by constructing stability maps [i.e., a 2D diagram that shows the regions of stable and unstable production of a well (Poblano et al. 2005; Fairuzov et al. 2004)]. The axes define the operating conditions in terms of the gas-injection rate and, for instance, the production-choke opening or wellhead pressure.

A dual gas lift well is a well with two independent tubings producing from two different hydrocarbon-bearing layers and sharing a common lift gas supply. The injection gas is supplied through a common casing and injected into the tubings through two individual gas lift valves. A sketch of a typical system is shown in **Fig. 1.** The dual gas lift well introduces a new instability phenomenon: the gas-distribution instability. This relates to the fact that under certain operating conditions, it is impossible to sustain the feed of injected gas into both tubings. Instead, all the injected gas will eventually be routed through one of the gas lift valves. As a consequence, the second tubing produces poorly or not at all, decreasing the total production substantially. There are few reports, if any, on automatic control of dual gas lift wells, although Boisard et al. (2002) briefly mentions an application.

In this paper, we present a simple, nonlinear dynamic model that captures the essential dynamics of the gas-distribution instability. It is an extension of the model for a single gas lift well presented in Eikrem et al. (2003) and Aamo et al. (2005). Using the model, we generate a stability map for a single-point dual gas lift well, and present a control structure for stabilizing the system at open-loop, unstable setpoints. The performance of the controller is demonstrated in simulations using the model, but more importantly, stabilization is also achieved in laboratory experiments.

This paper is organized as follows. In the Mathematical Model section, a nonlinear dynamic model applicable to dual gas lift wells is presented, followed by a discussion on instability mechanisms and the generation of stability maps in the Instability Mechanisms and Control section. The stability analysis is based on computing eigenvalues for the linearized model, accompanied by simulations using the nonlinear model. The proposed control structure is presented in the Automatic Control segment of that section, and experimental results using a gas lift laboratory located at the U. of Technology–Delft are shown in the Laboratory Experiments section. The paper ends with discussion and conclusions in the Conclusions section.

Mathematical Model

The process described in the Introduction and sketched in Fig. 1 is modeled mathematically by five states: x_1 is the mass of gas in the annulus; x_2 is the mass of gas in tubing 1; x_3 is the mass of oil above the gas-injection point in tubing 1; x_4 is the mass of gas in tubing 2; and x_5 is the mass of oil above the gas-injection point in tubing 2. Looking at Fig. 1, we have

$$\dot{x}_1 = w_{gc} - w_{iv,1} - w_{iv,2}, \quad (1)$$

$$\dot{x}_2 = w_{iv,1} + w_{rg,1} - w_{pg,1}, \quad (2)$$

$$\dot{x}_3 = w_{ro,1} - w_{po,1}, \quad (3)$$

$$\dot{x}_4 = w_{iv,2} + w_{rg,2} - w_{pg,2}, \quad (4)$$

and

$$\dot{x}_5 = w_{ro,2} - w_{po,2}. \quad (5)$$

where $^\bullet$ denotes differentiation with respect to time; w_{gc} is a constant mass flow rate of lift gas into the annulus; $w_{iv,k}$ is the mass flow rate of lift gas from the annulus into tubing k; $w_{rg,k}$ is the gas mass flow rate from the reservoir into tubing k; $w_{pg,k}$ is the mass flow rate of gas through production choke k; $w_{ro,k}$ is the oil mass flow rate from the reservoir into tubing k; and $w_{po,k}$ is the mass flow rate of produced oil through production choke k ($k \in \{1,2\}$). The flows are modeled by

$$w_{gc} = \text{constant flow rate of lift gas}, \quad (6)$$

$$w_{iv,1} = C_{iv,1}\sqrt{\rho_{a,i}\max\{0, p_{a,i} - p_{wi,1}\}}, \quad (7)$$

$$w_{iv,2} = C_{iv,2}\sqrt{\rho_{a,i}\max\{0, p_{a,i} - p_{wi,2}\}}, \quad (8)$$

$$w_{pc,1} = C_{pc,1}\sqrt{\rho_{m,1}\max\{0, p_{wh,1} - p_s\}}f_{pc,1}(u_1), \quad (9)$$

This paper (SPE 97731) received for review 23 March 2005. Revised manuscript received 17 June 2005. Paper peer approved 23 June 2005.

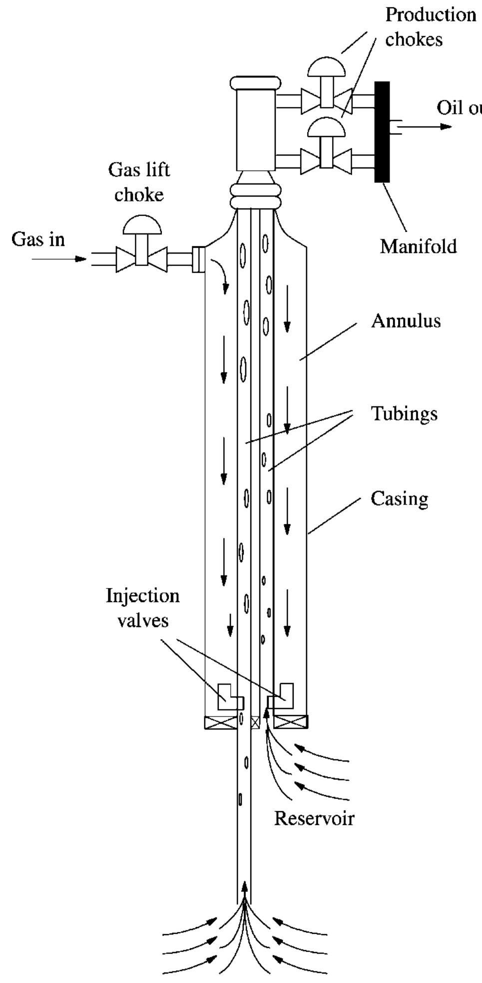

Fig. 1—A single-point dual gas lift oil well.

$$w_{pc,2} = C_{pc,2}\sqrt{\rho_{m,2}\max\{0, p_{t,2} - p_s\}}f_{pc,2}(u_2), \quad (10)$$

$$w_{pg,1} = \frac{x_2}{x_2 + x_3} w_{pc,1}, \quad (11)$$

$$w_{po,1} = \frac{x_3}{x_2 + x_3} w_{pc,1}, \quad (12)$$

$$w_{pg,2} = \frac{x_4}{x_4 + x_5} w_{pc,2}, \quad (13)$$

$$w_{po,2} = \frac{x_5}{x_4 + x_5} w_{pc,2}, \quad (14)$$

$$w_{ro,1} = f_{r,1}(p_{r,1} - p_{wb,1}), \quad (15)$$

$$w_{ro,2} = f_{r,2}(p_{r,2} - p_{wb,2}), \quad (16)$$

$$w_{rg,1} = r_{go,1} w_{ro,1}, \quad (17)$$

and

$$w_{rg,2} = r_{go,2} w_{ro,2}. \quad (18)$$

$C_{iv,k}$ and $C_{pc,k}$ are constants; u_k is the production choke setting [$u_k(t) \in (0,1)$]; $\rho_{a,i}$ is the density of gas in the annulus at the injection point; $p_{a,i}$ is the pressure in the annulus at the injection point; $\rho_{m,k}$ is the density of the oil/gas mixture at the wellhead; $p_{wh,k}$ is the pressure at the wellhead; $p_{wi,k}$ is the pressure in the tubing at the gas-injection point; $p_{wb,k}$ is the pressure at the wellbore; p_s is the pressure in the manifold; $p_{r,k}$ is the reservoir pressure far from the well; and $r_{go,k}$ is the gas-to-oil ratio (based on mass flows) of the flow from the reservoir. The function $f_{pc,k}$ is valve specific and represents a possibly nonlinear scaling of the flow as a function of the choke setting u_k. $f_{r,k}$ is a case-specific, possibly nonlinear, mapping from the pressure difference between the reservoir and the wellbore to the fluid flow from the reservoir. The manifold pressure, p_s, is assumed to be held constant by a control system, and the reservoir pressure, $p_{r,k}$, and gas-to-oil-ratio, $r_{go,k}$, are assumed to be slowly varying and are therefore treated as constant. Note that flow rates through the valves are restricted to be positive. The densities are modeled as follows:

$$\rho_{a,i} = \frac{M}{RT_a} p_{a,i}, \quad (19)$$

$$\rho_{m,k} = \frac{x_{1+k} = x_{2+k}}{L_{w,k} A_{w,k}}; \quad (20)$$

and the pressures as follows:

$$p_{a,i} = \left(\frac{RT_a}{V_a M} + \frac{gL_a}{V_a}\right) x_1, \quad (21)$$

$$p_{wh,k} = \frac{RT_{w,k}}{M} \frac{x_{1+k}}{L_{w,k} A_{w,k} - \nu_o x_{2+k}}, \quad (22)$$

$$p_{wi,k} = p_{wh,k} + \frac{g}{A_{w,k}}(x_{1+k} + x_{2+k}), \quad (23)$$

and

$$p_{wb,k} = p_{wi,k} + \rho_o g L_{r,k}. \quad (24)$$

M is the molar weight of the gas; R is the universal gas constant; T_a is the temperature in the annulus; $T_{w,k}$ is the temperature in the tubing; V_a is the volume of the annulus; L_a is the length of the annulus; $L_{w,k}$ is the length of the tubing; $A_{w,k}$ is the cross-sectional area of the tubing above the injection point; $L_{r,k}$ is the length from the reservoir to the gas-injection point; $A_{r,k}$ is the cross-sectional area of the tubing below the injection point; g is the gravity constant; ρ_o is the density of the oil; and ν_o is the specific volume of the oil. The oil is considered incompressible, so $\rho_o = 1/\nu_o$ is constant. The temperatures T_a and $T_{w,k}$ are slowly varying and, therefore, treated as constant. This model is an extension to a dual well from the single-well model presented in Eikrem et al. (2003) and Aamo et al. (2005).

Instability Mechanisms and Control

Casing-Heading Instability. The dynamics of highly oscillatory flow in single-point-injection gas lift wells can be described as follows:

- Gas from the annulus starts to flow into the tubing. As gas enters the tubing, the pressure in the tubing falls, accelerating the inflow of lift gas.
- If there is uncontrolled gas passage between the annulus and tubing, the gas pushes the major part of the liquid out of the tubing while the pressure in the annulus falls dramatically.
- The annulus is practically empty, leading to a negative pressure difference over the injection orifice, blocking the gas flow into the tubing. Because of the blockage, the tubing becomes filled with liquid and the annulus with gas.
- Eventually, the pressure in the annulus becomes high enough for gas to penetrate into the tubing, and a new cycle begins.

For more information on this type of instability, often termed severe slugging, refer to Xu and Golan (1989). The oscillating production associated with severe slugging causes problems for downstream processing equipment and is unacceptable in operations. The traditional remedy is to choke back to obtain a nonoscillating flow. As mentioned in the Introduction, automatic control is a powerful approach to eliminate oscillations; moreover, reports also show that this technology increases production (Kinderen et al. 1998; Jansen et al. 1999; Dalsmo et al. 2002; Boisard et al. 2002; Hu and Golan 2003; Eikrem et al. 2003; Aamo et al. 2005). Another approach is to fit a gas lift valve, which secures critical flow. This decouples the dynamics of the casing and tubing volumes and thereby eliminates casing-heading instabilities. Because the topic of this paper is a different kind of instability present in dual gas lift wells, refer to Kinderen et al. (1998), Jansen et al. (1999), Dalsmo et al. (2002), Boisard et al. (2002), Hu and Golan (2003) Eikrem et al. (2003), Aamo et al. (2005), and Xu and Golan

TABLE 1—NUMERICAL COEFFICIENTS		
Parameter	Value	Unit
M	0.028	kg/mol
R	8.31	J/Kmol
g	9.81	m/s^2
T_a	293	K
L_a	0.907	m
V_a	22.3×10^{-3}	m^3
ρ_o	1,000	kg/m^3
p_s	1×10^5	Pa
w_{gc}	0.6×10^{-3}	kg/s
$p_{r,1}$	2.9×10^5	Pa
$T_{w,1}$	293	K
$L_{w,1}$	14	m
$L_{r,1}$	4	m
$A_{w,1}$	0.314×10^{-3}	m^2
$A_{r,1}$	0.314×10^{-3}	m^2
$C_{iv,1}$	1.60×10^{-6}	m^2
$C_{pc,1}$	0.156×10^{-3}	m^2
$C_{r,1}$	12×10^{-6}	m^2
$r_{go,1}$	0	—
$p_{r,2}$	2.5×10^5	Pa
$T_{w,2}$	293	K
$L_{w,2}$	14	m
$L_{r,2}$	0	m
$A_{w,2}$	0.804×10^{-3}	m^2
$A_{r,2}$	0.804×10^{-3}	m^2
$C_{iv,2}$	2.80×10^{-6}	m^2
$C_{pc,2}$	0.156×10^{-3}	m^2
$C_{r,2}$	0.15×10^{-3}	m^2
$r_{go,2}$	0	—

(1989) for more details concerning stabilization of casing-heading instabilities.

Gas-Distribution Instability. In single-point dual gas lift oil wells another instability mechanism occurs that is related to the distribution of lift gas between the two tubings. The following statements assume subcritical flow between the annulus and the two tubings. Suppose each tubing is steadily drawing 50% of the lift gas. If one tubing momentarily draws more, the hydrostatic pressure drop in the tubing decreases, resulting in a larger pressure drop across the gas-injection orifice. This in turn accelerates the flow of gas, and the tubing draws even more lift gas. On the other hand, because the gas flow into the second tubing decreases, the hydrostatic pressure drop in the second tubing increases. Thus, the pressure drop across the gas-injection orifice decreases and, as a consequence, less gas is routed through the second tubing. Eventually, all lift gas will be routed through one tubing, which could impact total oil production.

We will now analyze gas-distribution instability using the relatively simple model (Eqs. 1 through 5), applied to the gas lift laboratory used in the experiments of the Laboratory Experiments section. For the laboratory, we have

$$f_{pc,k}(u_k) = 50^{u_k - 1} \qquad (25)$$

and

$$f_{r,k}(p_{r,k} - p_{wb,k}) = C_{r,k}\sqrt{\rho_o \max\{0, p_{r,k} - p_{wb,k}\}}, \qquad (26)$$

$k \in \{1,2\}$, where $C_{r,1}$ and $C_{r,2}$ are constants. **Table 1** summarizes the numerical coefficients used for this case. Given a pair of pro-

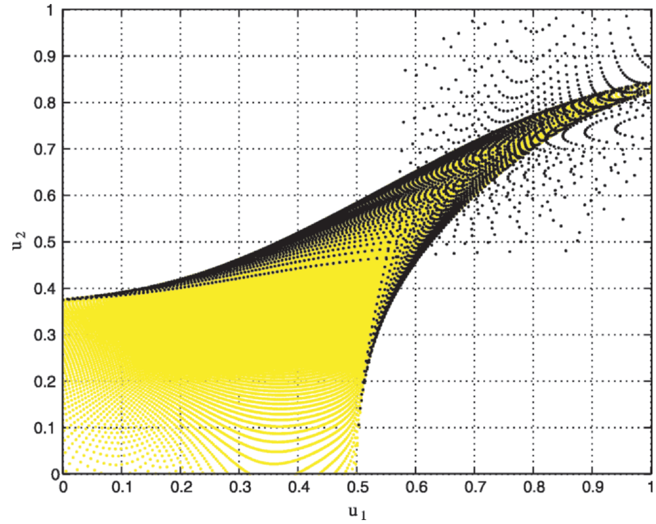

Fig. 2—Feasible choke settings for production from both tubings (yellow *and* black area) and choke settings for which open-loop production is unstable (black area).

duction-valve openings (u_1 and u_2 for the long and short tubing, respectively), we look for steady-state solutions by setting the time derivatives in Eqs. 1 through 5 to zero. Not all choices of u_1 and u_2 are feasible with respect to obtaining production from both tubings. The yellow *and* black dots in **Fig. 2** represent the pair u_1 and u_2 whose steady-state solution corresponds to production from both tubings. Other choices will give production from one tubing only and are not of interest to us. For the pairs of interest, we linearize the system of Eqs. 1 through 5 around the steady-state solution to study linear stability. The black dots in Fig. 2 represent (linearly) unstable settings. Roughly speaking, there is a region $(u_1,u_2) \in (0,0.50) \times (0,0.38)$ of linearly stable settings, while the rest are unstable settings. **Fig. 3** shows the steady-state total production as a function of (u_1,u_2). Clearly, production is higher for large values of u_1 and u_2. In fact, the optimum is located at approximately (1.00, 0.83), which corresponds to an unstable setting and a steady-state production substantially larger than what can be achieved in the linearly stable region. The gas distribution at steady state as a function of (u_1,u_2) is shown in **Fig. 4.**

For $u_1 = 0.90$ and $u_2 = 0.83$, the steady-state solution is unstable, with the largest real part of the eigenvalues of the linearized system being strictly positive $\{\max_j[\mathrm{Re}(\lambda_j)] = 0.03\}$. Selecting the initial condition equal to the steady-state solution, only slightly perturbed, and simulating the system of Eqs. 1 through 5, we obtain the result shown in **Figs. 5 and 6.** Fig. 5 shows the gas distribution between the two tubings as a function of time. At approximately steady state, five-sixths of the gas flows through the long tubing, while one-sixth of the gas flows through the short tubing. After approximately 2 minutes, the instability becomes visible in this graph and the gas starts to redistribute. After approximately 13 minutes, all the gas is routed through the short tubing. Fig. 6 shows the corresponding fluid-production curves. The long tubing has a substantial drop in production as a result of losing its lift gas, while the short tubing produces a little more. The total production drops approximately 20%.

Automatic Control. To optimize production, the instability needs to be dealt with. Motivated by the success of the controller used to stabilize the casing-heading instability, the control structure in **Fig. 7** is proposed. It consists of two independent feedback loops regulating the pressure at the injection points of each tubing. More precisely, two productivity-index (PI) controllers (proportional gain plus integral action) are employed, producing the incremental control signals:

$$\Delta u_k(j) = K_{c,k}\left[e_k(j) - e_k(j-1) + \frac{\Delta t}{\tau_{I,k}} e_k(j)\right], \qquad (27)$$

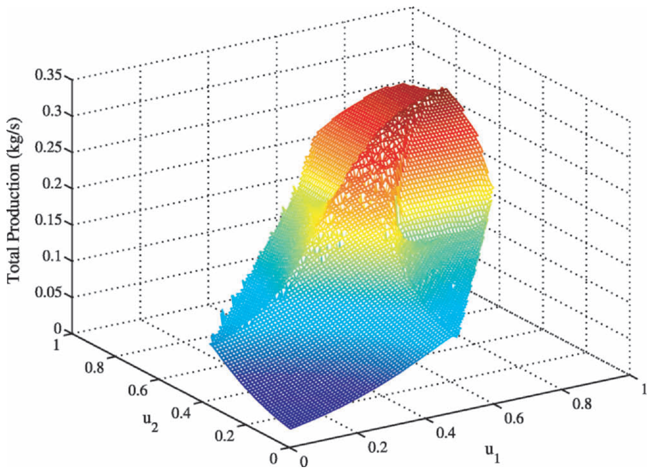

Fig. 3—Total fluid production as a function of u_1 and u_2.

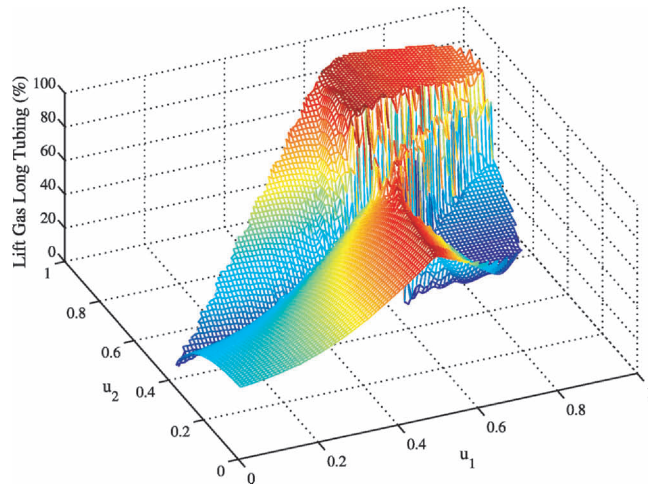

Fig. 4—Gas distribution as a function of u_1 and u_2.

$k \in \{1,2\}$, where

$$e_k(j) = p_{wi,k}(j) - p^*_{wi,k}. \quad (28)$$

$K_{c,k}$ and $\tau_{I,k}$ are the proportional gains and integral times, respectively; Δt is the sampling time; and j denotes the time index. $p^*_{wi,k}$, $k \in \{1,2\}$, are appropriate setpoints for the pressure. Repeating the simulation from Figs. 5 and 6, and closing the control loops at $t = 10$ minutes, we obtain the result in **Figs. 8 and 9.** Fig. 8 shows the gas distribution between the two tubings. At the time of initiation of control ($t = 10$ minutes), the gas has been considerably redistributed, but the control effectively drives the system back to the steady-state solution. Fig. 9 shows the corresponding fluid production. The control inputs that achieve this result are shown in **Fig. 10.**

Laboratory Experiments

Realistic tests of control structures for gas lift wells are performed using the gas lift well laboratory setup at Delft U. of Technology.* Prior laboratory experiments have verified that the PI controller (Eqs. 27 and 28) successfully stabilizes the casing-heading instability in single gas lift wells (Eikrem et al. 2003). Motivated by that result, the same control structure is tested experimentally for stabilization of the gas-distribution instability in dual gas lift wells.

Experimental Setup. The laboratory installation represents a dual gas lift well, using compressed air as lift gas and water as produced fluid. It is sketched in Fig. 7. The two production tubes are transparent, facilitating visual inspection of the flow phenomena occurring as control is applied. The long tubing measures 18 m in height and has an inner diameter of 20 mm, while the short tubing measures 14 m in height and has an inner diameter of 32 mm; see **Fig. 11a.** Each tubing has its own fluid reservoir represented by a tube of the same height, but with the substantially larger inner diameters of 80 mm and 101 mm, respectively. The reservoir pressures are given by the static height of the fluid in the reservoir tubes. The top of the tubings are aligned, which implies that the long tubing stretches 4 m deeper than the short one. A gas bottle represents the annulus (see Fig. 11b) with the gas-injection points located at the same level in both tubings and aligned with the bottom of the short production tube; see Fig. 7. In the experiments run in this study, gas is fed into the annulus at a constant rate of 0.6×10^{-3} kg/s. Input and output signals to and from the installation are handled by a microcomputer system (see Fig. 11c) to which a laptop computer is interfaced for running the control algorithm and presenting output.

Experimental Results. For the prescribed rate of lift gas, the two PI control loops sketched in Fig. 7 are incapable of stabilizing the

* The experimental setup is designed and implemented by Shell Intl. E&P, B.V., Rijswijk, and is now located in the Kramers Laboratorium voor Fysische Technologie, Faculty of Applied Sciences, Delft U. of Technology.

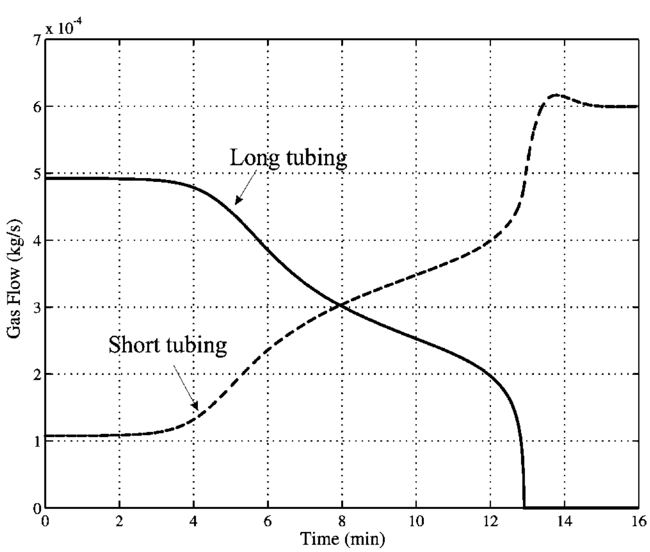

Fig. 5—Gas distribution as a function of time in the uncontrolled case.

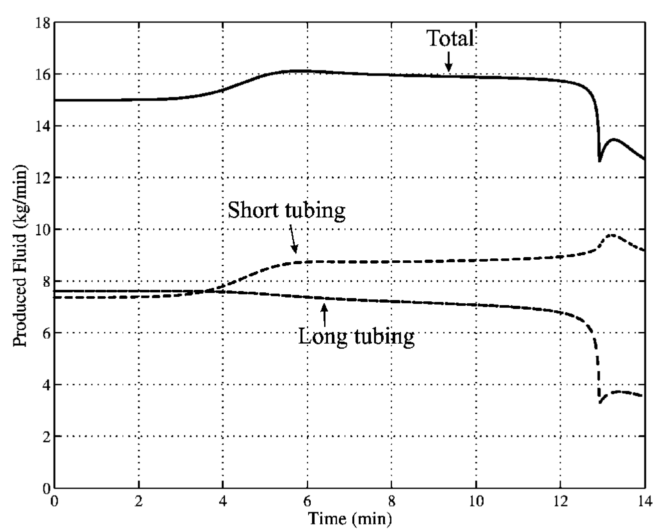

Fig. 6—Fluid production as a function of time in the uncontrolled case.

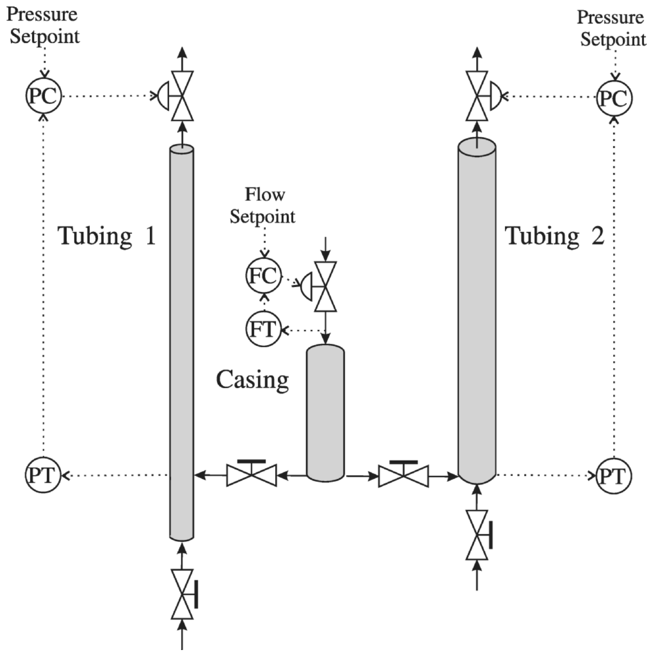

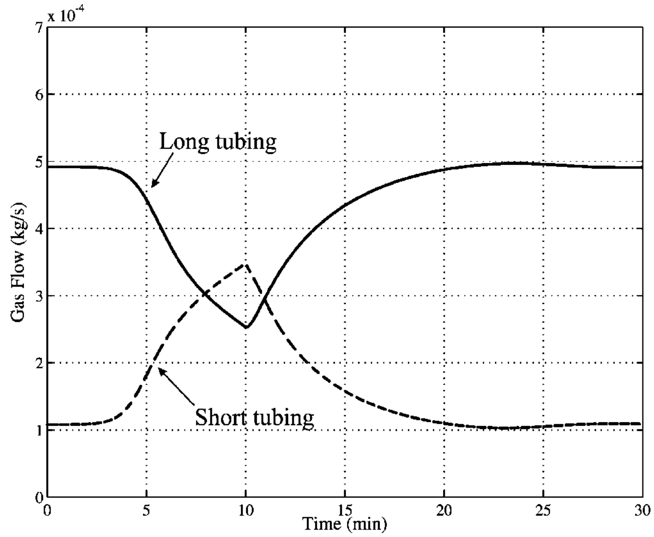

Fig. 8—Gas distribution as a function of time in the controlled case. Control is turned on at *t*=10 minutes.

Fig. 7—Controller structure for stabilization of the gas-distribution instability.

gas-distribution instability from an arbitrary initial condition and, in particular, initial conditions for which only one tubing is producing are not feasible. Therefore, a simple startup procedure consisting of the following steps was used to bring the system into a state from which the controller is able to stabilize:

1. Set u_1 and u_2 close to the expected steady-state values. This does not have to be very accurate.
2. Momentarily increase the rate of lift gas beyond the nominal rate (w_{gc}) such that both tubings draw gas and produce in open loop.
3. While both tubings draw lift gas, close the control loops.
4. Gradually decrease the rate of lift gas to its nominal value.

In the experiments, the coefficients for the controllers were set to $K_{c,1}=-1.2$, $K_{c,2}=-1.5$, and $\tau_{I,1}=\tau_{I,2}=50$ seconds, while the sampling time was $\Delta t=1.5$ seconds. The setpoints for $p_{wi,1}$ and $p_{wi,2}$ were set equal to $p^*_{wi,1}=p^*_{wi,2}=1$ barg (2 bara, 2×10^5 Pa), and the pressure deviations (28) were computed in barg (not in Pa). **Figs. 12 and 13** show the controlled downhole pressures $p_{wi,1}$ and $p_{wi,2}$ as functions of time, along with the setpoints $p^*_{wi,1}$ and $p^*_{wi,2}$. The two PI control loops gradually drive $p_{wi,1}$ and $p_{wi,2}$ toward their respective setpoints, reaching them in approximately 8 minutes. The commanded production-valve openings achieving this result are shown in **Figs. 14 and 15.** The valve openings are approximately 75 and 82%, respectively, when regulation to setpoint is achieved. At $t=10$ minutes, the control is turned off to demonstrate that the setpoints are indeed open-loop unstable. Figs. 12 and 13 show that the pressures diverge rapidly from their setpoints after $t=10$ minutes, confirming open-loop instability. **Fig. 16** shows the gas distribution between the two tubings. During regulation, in the period between $t=8$ and $t=10$ minutes, approximately one-third of the gas is routed through the short tubing while two-thirds are routed through the long tubing. The uneven gas distribution for this case of identical setpoints ($p^*_{wi,1}=p^*_{wi,2}$) is caused by the difference in valve characteristics between the two gas-injection valves (see $C_{iv,1}$ and $C_{iv,2}$ in Table 1). Total production during regulation is approximately 10 kg/min, as shown in **Fig. 17.** The effect of the gas-distribution instability is evident as control is turned off in the interval $t=10$ to $t=15$ minutes in Figs. 16 and 17. The gas quickly redistributes, with 100% being routed through the short tubing and nothing through the long tubing. As a consequence, the long tubing stops producing, while the short tubing produces a little more. The total production drops by approximately 28%, making a strong case for applying automatic

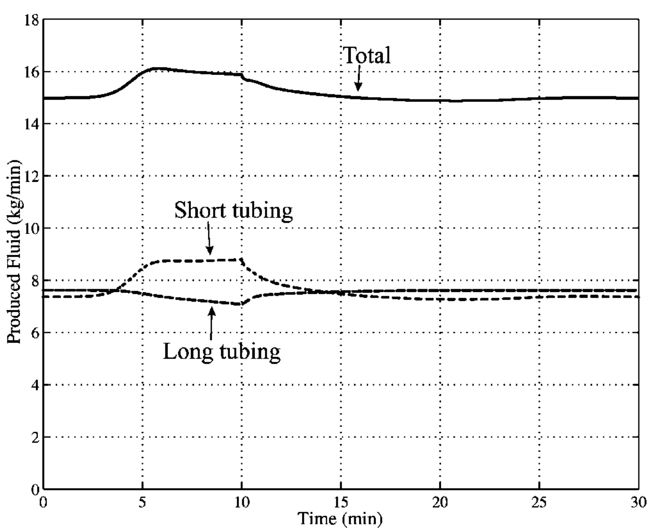

Fig. 9—Fluid production as a function of time in the controlled case. Control is turned on at *t*=10 minutes.

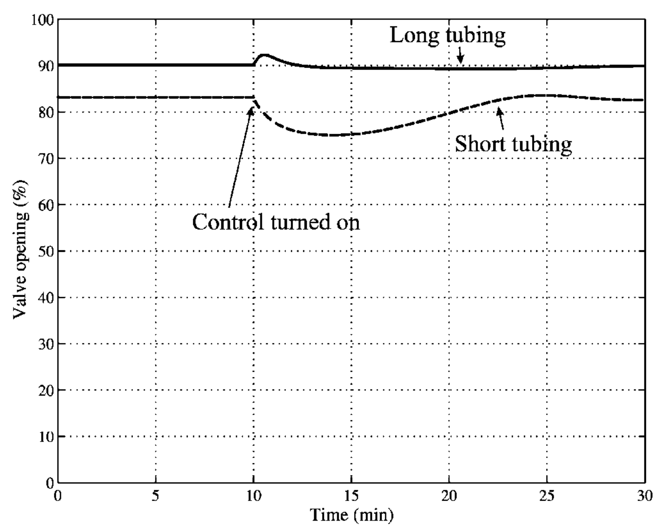

Fig. 10—Production-valve openings as functions of time. Control is turned on at *t*=10 minutes.

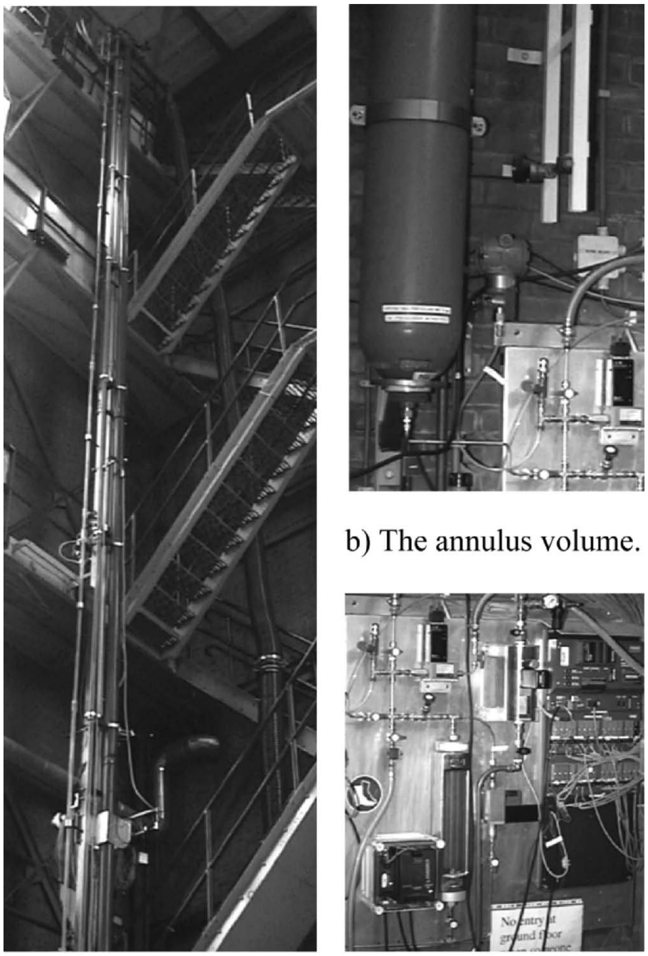

b) The annulus volume.

a) The production tubes. c) The microcomputer.

Fig. 11—The gas lift laboratory.

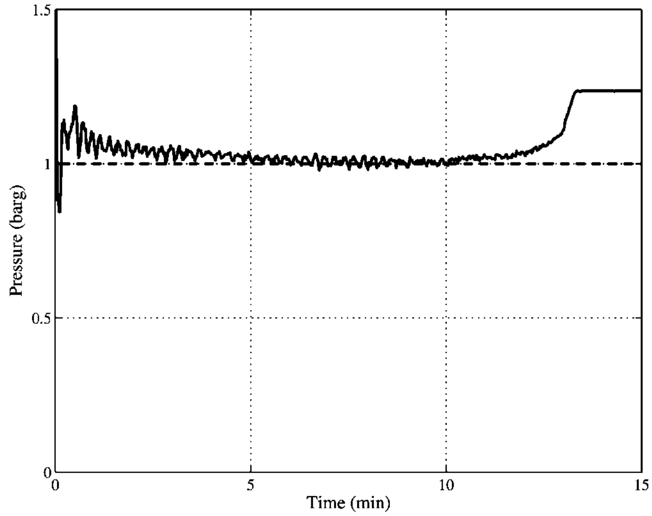

Fig. 12—Pressure at the location of gas injection in the long tubing. Control is turned off at t=10 minutes. The dashed line specifies the setpoint $p^*_{wi,1}$.

control. Comparing the interval $t \in (10,15)$ in Figs. 16 and 17 to Figs. 5 and 6, the qualitative resemblance is striking when considering the highly complex nature of two-phase flow and the simplicity of the model from the Mathematical Model section. While part of the difference between simulations and the experiments is caused by modeling error, the fact that simulations and experiments are performed at different setpoints is also a source of difference in this comparison. Although the model was set up for the laboratory case in this paper, it can easily be modified for real cases by changing parameters and reservoir flow relationships. In particular, $f_{r,1}(\cdot)$, $f_{r,2}(\cdot)$, $r_{go,1}$, and $r_{go,2}$ must be modified to model flows from a real reservoir. Typically, reservoir oil flow is modeled proportional (PI) to the pressure difference $p_{r,k}$–$p_{wb,k}$, while the gas-to-oil ratio is usually treated as constant.

Additional experiments were run to determine whether just one of the control loops is sufficient for stabilization of the gas-distribution instability. The experiments were unsuccessful, from which we conclude that both control loops are required. It is a drawback that the controllers rely on downhole measurements because such measurements may not be available or may be unreliable. The use of soft-sensing techniques may alleviate the need for downhole measurements, as demonstrated in Aamo et al. (2005). In that reference the downhole pressure was estimated on line from measurements at the wellhead only and the downhole-pressure estimates were employed for stabilization of the casing-heading instability.

Conclusions

In this paper, we have presented a simple scheme for stabilization of the gas-distribution instability in dual gas lift oil wells with a

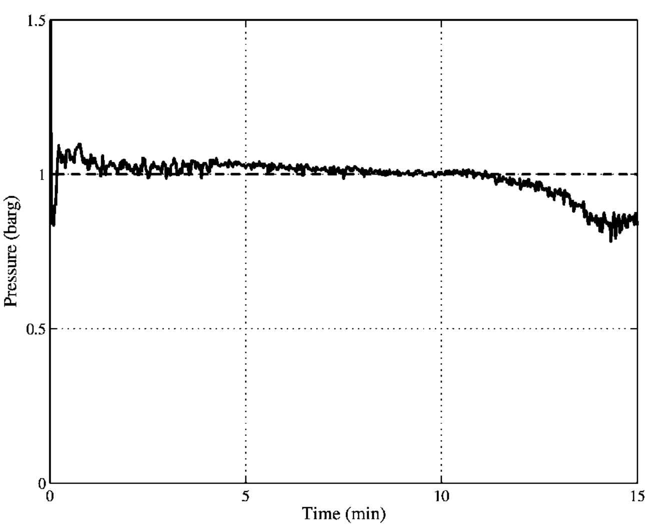

Fig. 13—Pressure at the location of gas injection in the short tubing. Control is turned off at t=10 minutes. The dashed line specifies the setpoint $p^*_{wi,2}$.

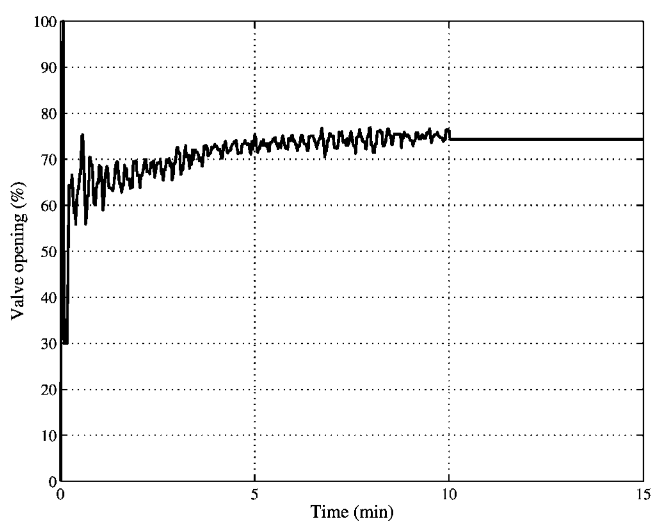

Fig. 14—Production-valve opening for the long tubing. Control is turned off at t=10 minutes, keeping the valve opening at the last controlled value.

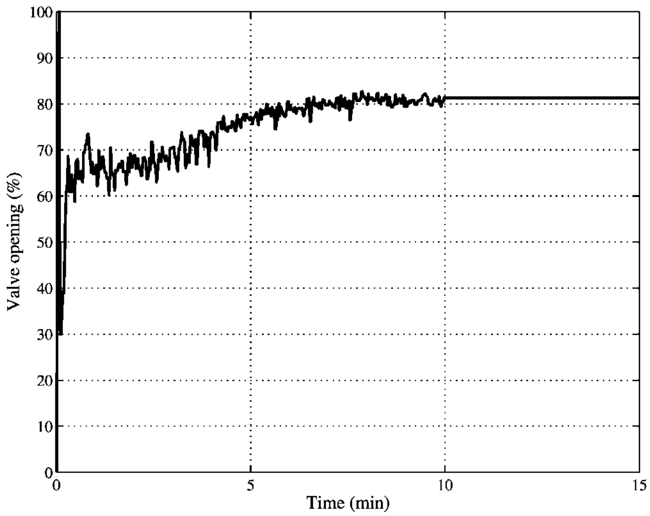

Fig. 15—Production-valve opening for the short tubing. Control is turned off at *t*=10 minutes, keeping the valve opening at the last controlled value.

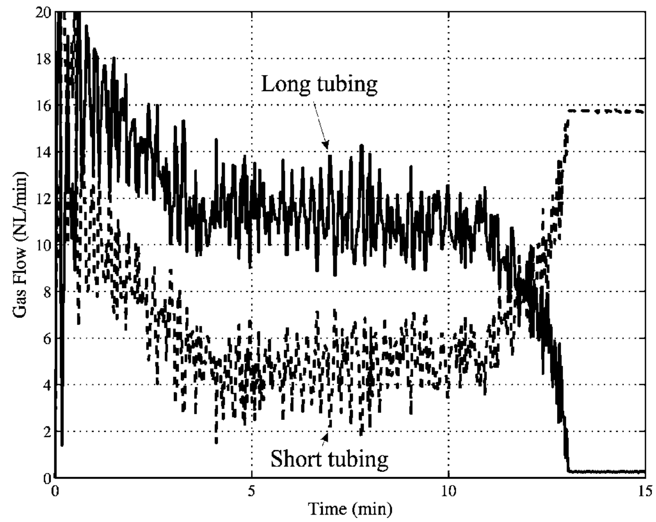

Fig. 16—Gas distribution as a function of time. Control is turned off at *t*=10 minutes.

common lift gas supply. A simple nonlinear dynamic model consisting of only five states was shown to successfully capture the essential dynamics of the gas-distribution instability, despite the complex nature of two-phase flow. Using the model, stability maps were generated showing regions of linearly stable and unstable settings for the production valves governing the produced flows from the two tubings. Accompanying plots of total production indicated that optimal steady-state production lies at large valve openings and well within the unstable region. A simple control structure was suggested that successfully stabilizes the gas-distribution instability in simulations and, more importantly, in laboratory experiments. For the settings used in the laboratory, total production dropped 28% when automatic control was switched off! Comparing simulation results with experiments, the predictive capability of the model is evident.

The results of this paper show that the problem of gas-distribution instability in dual gas lift oil wells may be analyzed and counteracted by simple methods and that there is a potential for significantly increasing production by installing a simple, inexpensive control system.

Acknowledgments

We gratefully acknowledge the support from Shell Intl. E&P, B.V., and Kramers Laboratorium voor Fysische Technologie, Faculty of Applied Sciences, Delft U. of Technology. In particular, we would like to thank Dr. Richard Fernandes (Shell) and Dr. R.V.A. Oliemans (Delft U. of Technology).

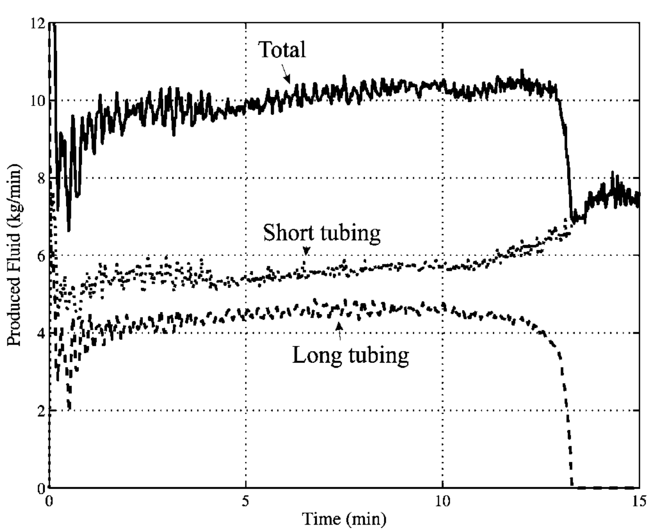

Fig. 17—Fluid production as a function of time. Control is turned off at *t*=10 minutes.

Nomenclature

$A_{r,1}$ = cross-sectional area of tubing 1 below the gas-injection point, $[L^2]$, m^2
$A_{r,2}$ = cross-sectional area of tubing 2 below the gas-injection point, $[L^2]$, m^2
$A_{w,1}$ = cross-sectional area of tubing 1 above the gas-injection point, $[L^2]$, m^2
$A_{w,2}$ = cross-sectional area of tubing 2 above the gas-injection point, $[L^2]$, m^2
$C_{iv,1}$ = valve constant for gas-injection valve 1, $[L^2]$, m^2
$C_{iv,2}$ = valve constant for gas-injection valve 2, $[L^2]$, m^2
$C_{pc,1}$ = valve constant for production valve 1, $[L^2]$, m^2
$C_{pc,2}$ = valve constant for production valve 2, $[L^2]$, m^2
$C_{r,1}$ = valve constant for reservoir valve 1, $[L^2]$, m^2
$C_{r,2}$ = valve constant for reservoir valve 2, $[L^2]$, m^2
e_k = regulation error, $[m/Lt^2]$, Pa
$f_{pc,1}$ = valve characteristic function
$f_{pc,2}$ = valve characteristic function
$f_{r,1}$ = production function, [m/t], kg/sec
$f_{r,2}$ = production function, [m/t], kg/sec
g = acceleration of gravity, $[L/t^2]$, m/sec^2
j = time index
$K_{c,1}$ = controller gain
$K_{c,2}$ = controller gain
L_a = length of annulus, [L], m
$L_{r,1}$ = length of tubing 1 below gas-injection point, [L], m
$L_{r,2}$ = length of tubing 2 below gas-injection point, [L], m
$L_{w,1}$ = length of tubing 1 above gas-injection point, [L], m
$L_{w,2}$ = length of tubing 2 above gas-injection point, [L], m
M = molar weight of gas, [m/n], kg/mol
p_a = pressure at the gas-injection point in the annulus, $[m/Lt^2]$, Pa
$p_{r,1}$ = pressure in reservoir 1, $[m/Lt^2]$, Pa
$p_{r,2}$ = pressure in reservoir 2, $[m/Lt^2]$, Pa
p_s = pressure in the manifold, $[m/Lt^2]$, Pa
$p_{wb,1}$ = pressure at wellbore 1, $[m/Lt^2]$, Pa
$p_{wb,2}$ = pressure at wellbore 2, $[m/Lt^2]$, Pa
$p_{wh,1}$ = pressure at wellhead 1, $[m/Lt^2]$, Pa
$p_{wh,2}$ = pressure at wellhead 2, $[m/Lt^2]$, Pa
$p_{wi,1}$ = pressure at gas-injection point in tubing 1, $[m/Lt^2]$, Pa

$p_{wi,2}$ = pressure at gas-injection point in tubing 2, [m/Lt^2], Pa
R = universal gas constant, [mL^2/nTt^2], J/Kmol
$r_{go,1}$ = gas-to-oil ratio in flow from reservoir 1
$r_{go,2}$ = gas-to-oil ratio in flow from reservoir 2
t = time, [t], seconds
T_a = temperature in annulus, [T], K
$T_{w,1}$ = temperature in tubing 1, [T], K
$T_{w,2}$ = temperature in tubing 2, [T], K
u_1 = setting of production valve 1
u_2 = setting of production valve 2
ν_o = specific volume of oil, [L^3/m], m^3/kg
V_a = volume of annulus, [L^3], m^3
w_{gc} = flow of gas into annulus, [m/t], kg/sec
$w_{iv,1}$ = flow of gas from annulus into tubing 1, [m/t], kg/sec
$w_{iv,2}$ = flow of gas from annulus into tubing 2, [m/t], kg/sec
$w_{pc,1}$ = flow of mixture from tubing 1, [m/t], kg/sec
$w_{pc,2}$ = flow of mixture from tubing 2, [m/t], kg/sec
$w_{pg,1}$ = flow of gas from tubing 1, [m/t], kg/sec
$w_{pg,2}$ = flow of gas from tubing 2, [m/t], kg/sec
$w_{po,1}$ = flow of oil from tubing 1, [m/t], kg/sec
$w_{po,2}$ = flow of oil from tubing 2, [m/t], kg/sec
$w_{rg,1}$ = flow of gas from reservoir into tubing 1, [m/t], kg/sec
$w_{rg,2}$ = flow of gas from reservoir into tubing 2, [m/t], kg/sec
$w_{ro,1}$ = flow of oil from reservoir into tubing 1, [m/t], kg/sec
$w_{ro,2}$ = flow of oil from reservoir into tubing 2, [m/t], kg/sec
x_1 = mass of gas in annulus, [m], kg
x_2 = mass of gas in tubing 1, [m], kg
x_3 = mass of oil in tubing 1, [m], kg
x_4 = mass of gas in tubing 2, [m], kg
x_5 = mass of oil in tubing 2, [m], kg
Δt = timestep, [t], seconds
$\Delta u_k(j)$ = valve opening change, [-]
$\rho_{a,i}$ = density of gas at injection point in annulus, [m/L^3], kg/m^3
$\rho_{m,1}$ = density of mixture at wellhead 1, [m/L^3], kg/m^3
$\rho_{m,2}$ = density of mixture at wellhead 2, [m/L^3], kg/m^3
ρ_o = density of oil, [m/L^3], kg/m^3
$\tau_{I,k}$ = integral time, [t], sec
λ_j = eigenvalue

References

Aamo, O.M., Eikrem, G.O., Siahaan, H., and Foss, B.A. 2005. Observer Design for Multiphase Flow in Vertical Pipes with Gas Lift—Theory and Experiments. *J. of Process Control* **15** (1): 247–257.

Boisard, O., Makaya, B., Nzossi, A., Hamon, J.C., and Lemetayer, P. 2002. Automated Well Control Increases Performance of Mature Gas-Lifted Fields, Sendji Case. Paper SPE 78590 presented at the SPE Abu Dhabi International Petroleum Exhibition and Conference, Abu Dhabi, 13–16 October.

Dalsmo, M., Halvorsen, E., and Slupphaug, O. 2002. Active Feedback Control of Unstable Wells at the Brage Field. Paper SPE 77650 presented at the SPE Annual Technical Conference and Exhibition, San Antonio, Texas, 29 September–2 October.

Eikrem, G.O., Imsland, L., and Foss, B. 2003. Stabilization of Gas Lifted Wells Based on State Estimation, *Proc.* of the 2003 IFAC Intl. Symposium on Advanced Control of Chemical Processes, Hong Kong, 11–14 January.

Fairuzov, Y.V., Guerrero-Sarabia, I., Calva-Morales, C. et al. 2004. Stability Maps for Continuous Gas-Lift Wells: A New Approach to Solving an Old Problem. Paper SPE 90644 presented at the SPE Annual Technical Conference and Exhibition, Houston, 26–29 September.

Hu, B. and Golan, M. 2003. Gas Lift Instability Resulted Production Loss and Its Remedy by Feedback Control: Dynamical Simulation Results. Paper SPE 84917 presented at the SPE International Improved Oil Recovery Conference in Asia Pacific, Kuala Lumpur, 20–21 October.

Jansen, B., Dalsmo, M., Nøkleberg, L., Havre, K., Kristiansen, V., and Lemetayer, P. 1999. Automatic Control of Unstable Gas Lifted Wells. Paper SPE 56832 presented at the SPE Annual Technical Conference and Exhibition, Houston, 3–6 October.

Kinderen, W.J.G.J., Dunham, C.L., and Poulisse, H.N.J. 1998. Real-Time Artificial Lift Optimization. Paper SPE 49463 presented at the SPE Abu Dhabi International Petroleum Exhibition and Conference, Abu Dhabi, 11–14 November.

Poblano, E., Camacho, R., and Fairuzov, Y.V. 2005. Stability Analysis of Continuous-Flow Gas Lift Wells. *SPEPF* **20** (1): 70–79. SPE 77732.

Xu, Z.G. and Golan, M. 1989. Criteria for Operation Stability of Gas Lift Wells. Unsolicited paper SPE 19362 available at www.spe.org.

SI Metric Conversion Factors

bar ×	1.0*	E+05	=	Pa
bbl ×	1.589 873	E–01	=	m^3
Btu ×	1.055 056	E+00	=	kJ
ft ×	3.048*	E–01	=	m
ft^2 ×	9.290 304*	E–02	=	m^2
ft^3 ×	2.831 685	E–02	=	m^3
°F	(°F+459.67)/1.8		=	K
kg/ m^3 ×	1.601 846	E+01	=	lbm/ ft^3
lbm ×	4.535 924	E–01	=	kg

*Conversion factor is exact.

Gisle Otto Eikrem is currently working towards a PhD degree in engineering cybernetics at the Norwegian U. of Science and Technology (NTNU). His research interests include process control, with special emphasis on flow assurance. He holds an MSc degree in chemical engineering from NTNU. **Ole Morten Aamo** was a post-doctoral fellow at the Marine Technology Dept. at NTNU from 2002 to 2003 and now holds a post-doctoral position at the Engineering Cybernetics Dept. He is a coauthor of the book *Flow Control by Feedback* (published by Springer-Verlag in 2002). His research interests include control of distributed-parameter systems, with special emphasis on fluid flows and applications in the petroleum industry. Aamo holds MSc and PhD degrees in engineering cybernetics from NTNU. **Bjarne A. Foss** currently leads the Gas Technology Center NTNU-SINTEF. He has been a professor at the Engineering Cybernetics Dept. at NTNU since 1989. He has also been a visiting professor at the U. of Texas at Austin. His main interests are in control theory and applications within the process and petroleum-related industries. He is a cofounder of two companies: Cybernetica AS and Cyberlab.org AS. Foss holds a PhD from NTNU. He is a senior member of IEEE, an associate editor of *J. of Process Control,* and a member of The Norwegian Academy of Technical Sciences.